ORGANOMETALLICS

Article

pubs.acs.org/Organometallics

Intermolecular Alkyne Hydroacylation. Mechanistic Insight from the Isolation of the Vinyl Intermediate That Precedes Reductive Elimination

Rebekah J. Pawley,[†] Miguel A. Huertos,[†] Guy C. Lloyd-Jones,[‡] Andrew S. Weller,*[,†] and Michael C. Willis[†]

[†]Department of Chemistry, Inorganic Chemistry Laboratories, South Parks Road, University of Oxford, Oxford, U.K. OX1 3QR

[‡]School of Chemistry, University of Bristol, Cantocks Close, Bristol, U.K. BS8 1TS

Supporting Information

ABSTRACT: The isolation of the branched alkenyl intermediate that directly precedes reductive elimination of the final α,β-unsaturated ketone product is reported for the hydroacylation reaction between the alkyne HC≡CAr^F (Ar^F = 3,5-$(CF_3)_2C_6H_3$) and the β-S-substituted aldehyde 2-(methylthio)benzaldehyde: [Rh(*fac*-κ^3-DPEphos)(C(=CH_2)-Ar^F)(C(O)C_6H_4SMe)$_2$][$CB_{11}H_{12}$]. The structure of this intermediate shows that, in this system at least, hydride migration rather than acyl migration occurs. Kinetic studies on the subsequent reductive elimination to form the crystallographically characterized ketone-bound product [Rh(*cis*-κ^2-DPEphos)(η^2:η^2,κ^1-H_2C=C(Ar^F)C(=O)(C_6H_4SMe)]-[$CB_{11}H_{12}$] yield the following activation parameters for reductive elimination, which follows first-order kinetics (k_{obs} = (6.14 ± 0.04) × 10^{-5} s^{-1}, 324 K): $\Delta H^{\ddagger}$ = 95 ± 2 kJ mol^{-1}, $\Delta S^{\ddagger}$ = −32 ± 7 J K^{-1} mol^{-1}, $\Delta G^{\ddagger}$(298 K) = 105 ± 4 kJ mol^{-1}. Mechanistic studies, including selective deuteration experiments, show that hydride insertion is not reversible and also reveal that an interesting isomerization process is occurring between the two branched alkenyl protons that is suggested to occur via a metallocyclopropene intermediate. During catalysis, the consumption of substrates and evolution of products follow pseudo zero-order kinetics. The observation of both linear and branched products under stoichiometric and catalytic regimes, in combination with kinetic modeling, allows for an overall mechanistic scheme to be presented. Partitioning of linear and branched pathways at the hydride insertion step occurs with an approximate 2:1 selectivity, while reductive elimination of the linear product is at least 3 orders of magnitude faster than that from the branched. An explanation for the large difference in rate of reductive elimination in this system, as recently outlined by Goldman, Krogh-Jespersen, and Brookhart, is that steric crowding in branched intermediates can slow C−C reductive elimination even though such species are higher in energy than their linear analogues, if the rotation of the vinyl group to the appropriate orientation is inhibited by steric crowding in the branched isomers.

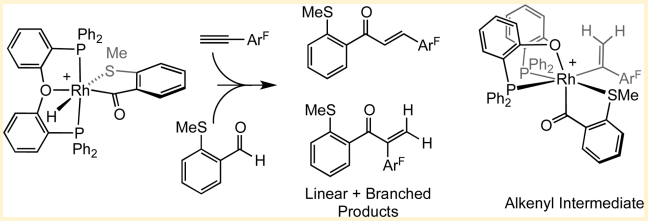

INTRODUCTION

The hydroacylation reaction is an attractive synthetic methodology to prepare ketones from aldehydes and alkenes or alkynes in an atom-efficient manner using widely available starting materials.[1−4] The reaction combines the C−H activation of an aldehyde with a C−C bond-forming step and is often promoted by rhodium phosphine catalysts (e.g., **A**, Chart 1) using β-substituted chelating aldehydes as substrates,[5,6] although other notable catalyst systems have been reported.[7−10] Significant advances have been made in developing this transformation with regard to overall catalyst activities (e.g., **B** and **C**),[7,8,11,12] attenuation of catalyst deactivation by decarbonylation using hemilabile ligands (e.g., **D**),[13,14] control over linear/branched ratios (e.g., **E**),[9,10,15−18] broad alkene/alkyne scope,[11] and enantioselective control.[16,19−21] However, the development of intermolecular hydroacylation using simple, nonchelating aldehydes lags behind,[7,8,12,21,22] due to the combined problems of C−H activation of the aldehyde and irreversible reductive decarbonylation from the resulting acyl hydride intermediate. Central to the delivery of a truly general hydroacylation reaction is a fundamental understanding and manipulation of the complete catalytic cycle for a broad range of substrates.

Mechanistic studies on a number of selected of systems,[5,7,8,11,13,18,23,24] coupled with computational investigations,[25−27] support oxidative addition of the aldehyde to give an acyl hydride being the first productive step, followed by alkene (or alkyne) coordination (Scheme 1). Migratory insertion of the hydride, rather than the acyl,[28−31] is then proposed to occur to give an unobserved acyl alkyl (alkenyl) intermediate as either linear (1,2-insertion) or branched (2,1-insertion) regioisomers. Studies on alkene hydroacylation have shown that all these steps can be reversible.[5,7,11,12,18,23,24,32] Reductive elimination from the putative acyl alkyl (or alkenyl) intermediate is irreversible, however, and is suggested to be the turnover-limiting step in alkene hydroacylation.[5,7,12,24] Interest-

Received: July 11, 2012
Published: July 26, 2012

   dx.doi.org/10.1021/om300647n | *Organometallics* 2012, 31, 5650−5659

Chart 1. [a]

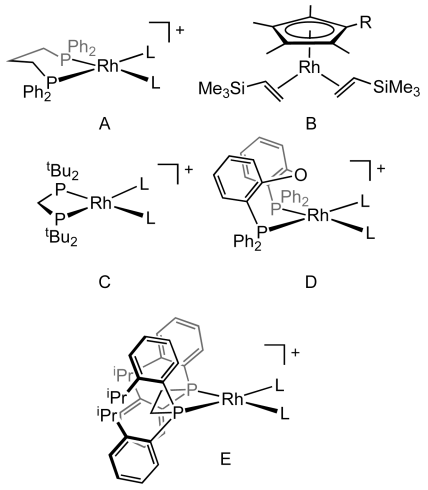

[a]L = solvent (e.g. acetone). Anions are not shown.

ingly, Dong has reported that for intramolecular *aldehyde* hydroacylation the insertion step is turnover limiting.[23] Studies on alkene hydroacylation systems suggest that it is the relative barrier to reductive elimination from the linear (or branched) acyl alkyl that controls the final selectivity.[7,11] We have recently reported that the linear/branched selectivity in hydroacylation of electron-poor alkynes with *β*-S-substituted aldehydes can be controlled using bulky ortho-substituted dppe-derived ligands and, in particular, $(o\text{-}^{i}PrC_6H_4)_2PCH_2CH_2P(o\text{-}^{i}PrC_6H_4)_2$ ligated to a cationic Rh center (**E**, Chart 1), suggesting that ortho substituents force a conformation of the phosphine/aryl groups in the alkenyl/acyl intermediates that encourages reductive elimination of the branched intermediate over linear.[18] Ligands that are usually linear selective in hydroacylation such as DPEphos, however, show poor linear selectivity with electron-poor alkynes and aryl aldehydes. This regioselectivity issue has recently been resolved by use of the electron-rich chelating phosphine ligand $Cy_2PCH_2CH_2PCy_2$, which allows for efficient linear-selective alkyne hydroacylation reactions between a wide range of aldehydes and alkynes.[33] We have also reported that selectivity for alkene versus aldehyde hydroacylation can be influenced by the nature of the chelating ligand, which is suggested to influence the relative barriers of migratory insertion and reductive elimination.[34] In intramolecular systems, linear/branched selectivity can arise from the preferential formation of five-membered rhodacycles on hydride insertion.[17]

Given this interest in the mechanism, and the benefits in overall substrate scope that come from its study, definitive examples of the observation of intermediates that directly precede the turnover-limiting (and potentially product selecting) step of reductive elimination to form the final ketone product are limited. Brookhart has measured the rate of reductive elimination in Co[12] and Rh[7] complexes derived from precatalysts exemplified by **B**. The resting states for these systems are alkyl/aryl carbonyl complexes, which precede the acyl-alkyl intermediates required for reductive elimination. We have also reported the spectroscopic observation of a short-lived acyl-alkyl intermediate in the hydroacylation reaction of methyl acrylate and the *β*-S-substituted aldehyde 2-(methylthio)benzaldehyde (**1a**), using the DPEphos catalyst system (**D**), but no kinetic data were obtained.[13]

The synthesis of intermediates prior to reductive elimination for the most general class of catalysts used for hydroacylation, [Rh(chelating phosphine)]$^+$, would give important structural and mechanistic data pertinent to C−C bond formation and linear/branched selectivity, and would also determine whether hydride migration or acyl migration (carbometalation[35]) occurs—questions that have only been addressed computationally.[23,25−27] As far as we are aware, such intermediates have not been experimentally reported for *alkyne* hydroacylation. Tanaka and Fu have reported mechanistic details of intramolecular alkynal hydroacylation, but no intermediates were isolated.[36−38]

We report here the synthesis and onward reactivity of such an intermediate, isolated using the hemilabile[39,40] DPEphos catalyst system, aldehyde **1a**, and the electron-deficient alkyne $HC{\equiv}CAr^F$ (Ar^F = 3,5-$(CF_3)_2C_6H_3$) (**2**; Chart 2); this combination was deliberately chosen, as it gives a mixture of linear and branched products.[33] The isolation of such an intermediate allows us to probe the rate of reductive elimination of final product, isomerization processes, and also the regioselectivity of intermolecular alkyne hydroacylation to give the corresponding linear (**4**) and branched (**5**) products (Chart 2).

RESULTS

Synthesis of the Branched Intermediate. Addition of *β*-substituted aldehyde **1a** (1 equiv) to a d_6-acetone solution of [Rh(*cis*-*κ*^{2}-DPEphos)(acetone)$_2$][$CB_{11}H_{12}$][41] forms the previ-

Scheme 1. General Mechanism for Hydroacylation using the $[RhL_2]^+$ System

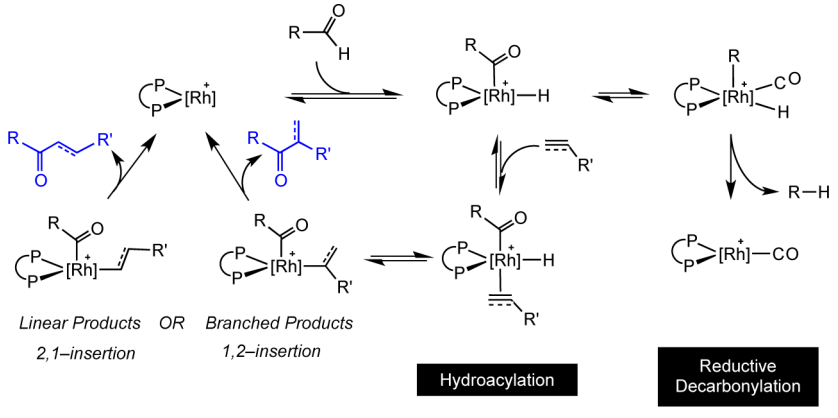

dx.doi.org/10.1021/om300647n | *Organometallics* 2012, 31, 5650−5659

Chart 2

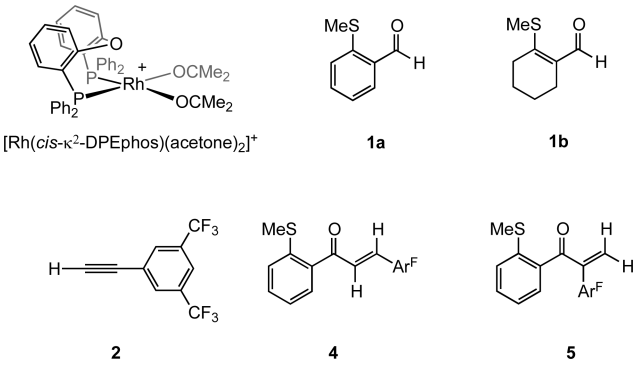

ously reported acyl hydride complex [Rh(*mer*-κ^3-DPEphos)(H)(C(O)C_6H_4SMe)][$CB_{11}H_{12}$] (**3a**)[13,41] in quantitative yield by NMR spectroscopy (Scheme 2). The analogous complex with the alkenyl SMe-substituted aldehyde 2-(methylthio)-cyclohex-1-enecarbaldehyde (**1b**), [Rh(*mer*-κ^3-DPEphos)(H)(C(O)C_6H_8SMe)][$CB_{11}H_{12}$] (**3b**), was also prepared (Supporting Information). Addition of 1 equiv of alkyne **2** to **3a** resulted in a reproducible mixture of five organometallic complexes, as determined by $^{31}P\{^1H\}$ NMR spectroscopy. As we will show later, these complexes were identified as a mixture of linear and branched hydroacylation derived products bound to the metal center, in which the partition ratio is ~2:1 in favor of the linear. In contrast, the addition of an excess (5 equiv) each of **1a** and **2** to [Rh(*cis*-κ^2-DPEphos)(acetone)$_2$][$CB_{11}H_{12}$] (298 K, 1 h) ultimately resulted in the clean formation of a single organometallic component that could be isolated in very good yield (86%). NMR spectroscopy and a single-crystal X-ray diffraction study showed the organometallic product to be [Rh(*fac*-κ^3-DPEphos)(C(=CH_2)Ar^F)(C(O)C_6H_4SMe)$_2$][$CB_{11}H_{12}$] (**6**). Also formed under these conditions was approximately 2 equiv of the linear hydroacylation product **4** in addition to unreacted **1a** and **2**. Thus, it appears that there is an average of approximately 2 turnovers to produce linear **4**, but once branched **6** is formed (which must undergo reductive elimination of product far more slowly at 298 K), the reaction slows considerably. Consistent with this, none of the branched product **5** was observed by NMR spectroscopy under these conditions of time and temperature. Under these conditions we propose that **3a** is initially formed, and starting from preformed **3a**[13] gave the same distribution of products on addition of excess **1a** and **2**.

The solid-state structure of **6** is shown in Figure 1, which demonstrates that the alkyne has undergone insertion into the

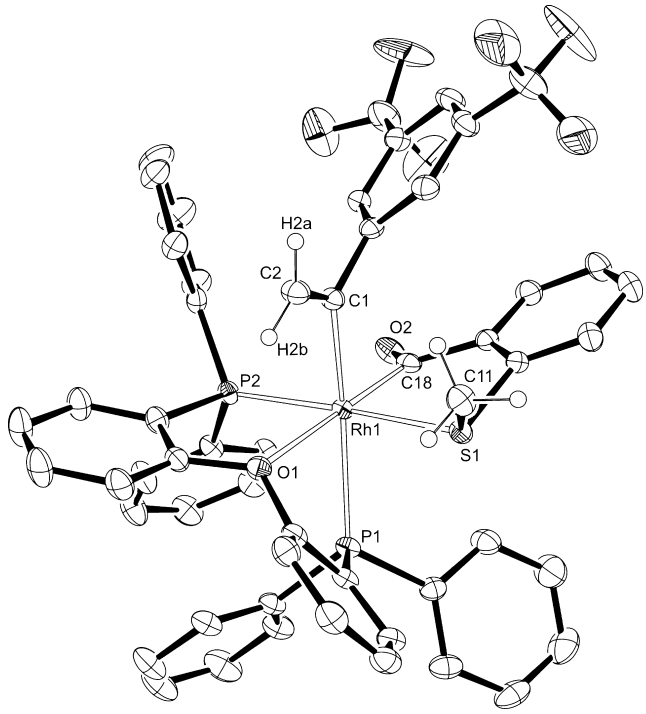

Figure 1. Displacement ellipsoid plot (30% probability) of complex **6**. Selected bond lengths (Å) and angles (deg): Rh1−P1, 2.4542(7); Rh−P2, 2.2953(7); Rh1−O1, 2.3458(17); Rh1−C18, 1.977(3); Rh1−S1, 2.3757(7); Rh1−C1, 2.097(3); C1−C2, 1.327(4); C18−O2, 1.212(3); C1−Rh1−P1, 162.90(7); P2−Rh1−S1, 175.17(2); O1−Rh1−C18, 179.50(9); P1−Rh1−P2, 95.41(2). The anion and the majority of the H atoms are not shown.

hydride ligand present in **3a** to give the branched acyl-alkenyl complex, rather than the linear complex. The DPEphos ligand in **6** adopts a *fac*-κ^3 coordination mode, with the central oxygen lying *trans* to the high *trans* influence acyl ligand. The Rh−O distance reflects this (2.3458(17) Å), being longer than that in **3a** (2.248(3) Å, as the $CB_{11}H_6Cl_6$ salt[13]), in which the DPEphos adopts a *mer*-κ^3 coordination geometry. The alkenyl group sits *cis* to the acyl and *trans* to one phosphine (P1). As expected from *trans* influence arguments the Rh−P1 distance is longer compared to Rh−P2 (2.4542(7) and 2.2953(7) Å, respectively). The C1−C2 distance (1.327(4) Å) is similar to

Scheme 2

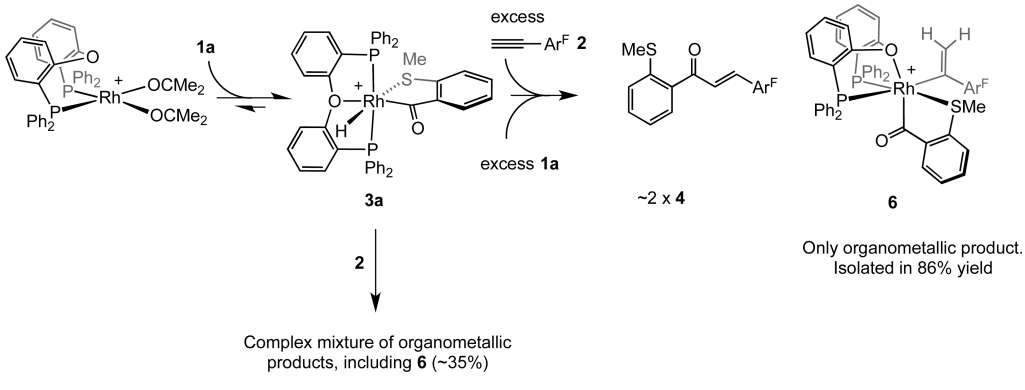

dx.doi.org/10.1021/om300647n | *Organometallics* 2012, 31, 5650−5659

Scheme 3

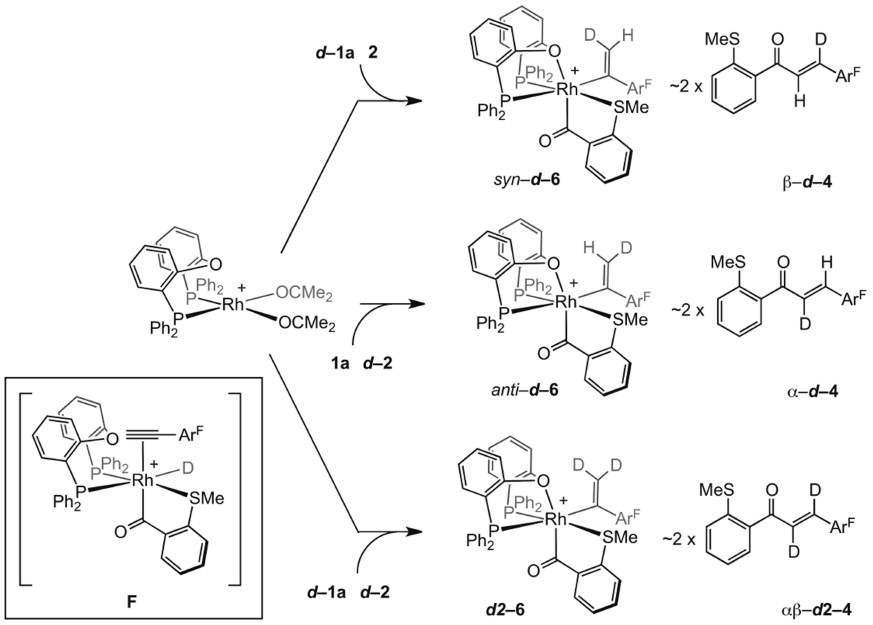

Scheme 4

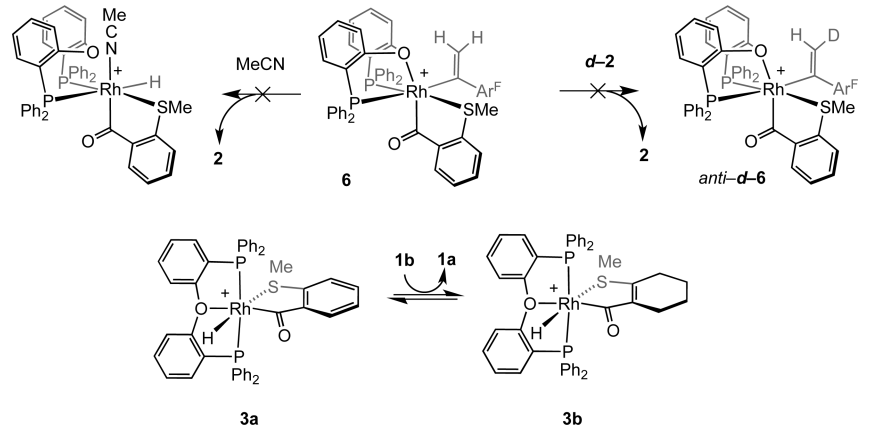

those found in other branched alkenyl complexes: (PCP)Ir(PhC═CH_2)(CCPh)(CO) (1.343(3) Å; PCP = κ^3-C_6H_3-2,6-($CH_2P^tBu_2$)$_2$)[42] and (PCP′)Ru(PhC═CH_2)Cl (1.322(6) Å; PCP′ = *N*,*N*′−bis(diisopropylphosphino)dipyrromethane).[43] The alkenyl group is directed along the Rh1−O1 vector; dihedral angle C2C1/Rh1O1 = 8.9°.

In solution a pair of doublets of doublets are observed in the $^{31}P\{^1H\}$ NMR spectrum at δ 21.9 and 13.1, with differing $^{31}P-^{103}Rh$ coupling constants (167 and 79 Hz, respectively). The smaller of the two couplings places the associated phosphorus (δ 13.1) *trans* to the alkenyl ligand. Confirmation of this arrangement comes from the $^1H\{^{31}P\}$ HMBC experiment that shows a strong correlation between S*Me* and the phosphorus signal at δ 21.9, which places these groups mutually *trans* to one another. Similar correlations have been observed previously in acyl hydride complexes.[13,34] The ^1H NMR spectrum shows a featureless hydride region and two slightly broadened doublets at δ 5.72 (J(PH) = 9 Hz) and δ 5.50 (J(PH) = 18 Hz), that are assigned to the 1,1-alkenyl and correlate to one another in the $^1H/^1H$ COSY spectrum. These alkenyl chemical shifts are close to those reported in (PCP)Ir(PhC═CH_2)(CCPh)(CO).[42] An HSQC experiment shows that these two signals are associated with a single ^{13}C environment (δ 122.2). A $^1H\{^{31}P$-selective$\}$ NMR experiment demonstrates that the doublet structure in both signals comes from coupling to the single ^{31}P environment at δ 13.1, and on the basis of the relative J(PH) coupling constant we assign the signal at δ 5.50 to the geminal hydrogen *anti* to P1, i.e. H2a, as this shows the largest coupling, as noted previously in 1,1-alkenyl systems of Pd diphosphines.[44] The ^{19}F NMR spectrum shows a single environment (δ 62.9), suggesting free rotation of the alkenyl arene group. These data do not allow us to comment upon restricted rotation around the Rh−C1 bonds, although such behavior has been noted to occur in a number of examples of branched alkenyl complexes.[42,45,46] These NMR data are all consistent with a structure in solution that is very close to that observed in the solid state.

Deuteration experiments using excess **1a**/***d*-1a** or **2**/***d*-2** with [Rh(*cis*-κ^2-DPEphos)(acetone)$_2$][$CB_{11}H_6Br_6$] at 298 K reveal that the formation of **6** occurs by insertion of the hydride with the expected[46] *cis* stereochemistry (Scheme 3), presumably via an unobserved intermediate such as **F**. Thus, addition of ***d*-1a**/**2** results in the formation of *syn*-***d*-6** in which the proton *syn* to P1, H2b, is replaced with D (i.e., an absence of the signal δ 5.72

dx.doi.org/10.1021/om300647n | *Organometallics* 2012, 31, 5650−5659

Scheme 5

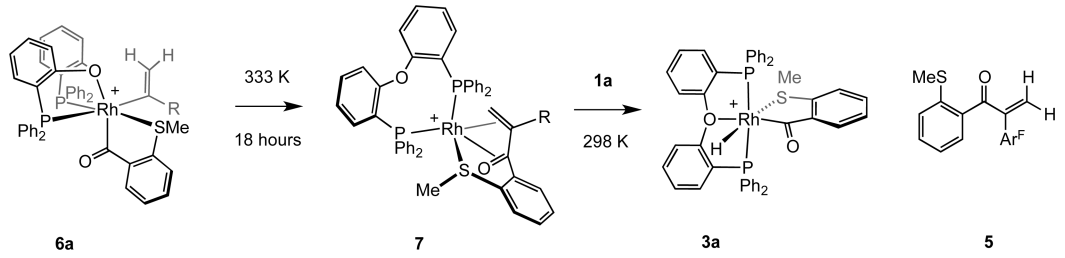

in the ^{1}H NMR spectrum). Addition of **1a**/***d*-2** reveals selective D incorporation into the *anti* position, H2a, to give *anti*-***d*-6**. Addition of ***d*-1a**/***d*-2** results in complete H/D exchange in the alkenyl, to form ***d*$_2$-6**. ^{2}H NMR spectroscopy confirms all these observations. Approximately 2 equiv of the corresponding deuterated linear product, **4**, is also observed in each of these reactions, being formed in >99% selectivity of D incorporation, with no scrambling into other positions (Scheme 3). Unreacted aldehyde and alkyne are also observed. Addition of ***d*-2** to **6** (323 K, 12 h) resulted in essentially no H/D exchange (less than 5%), with **7** (vide infra) observed as the final organometallic product.[47] This rules out significant reversible alkyne insertion coupled with alkyne exchange. Similar observations have been made for (PCP′)Ru(PhC═CH$_2$)Cl,[43] whereas in contrast (PCP)Ir(PhC═CH$_2$)(CCPh) does undergo this exchange.[42] Further evidence against reversible insertion is given that addition of MeCN to **6** does not generate the previously reported complex [Rh(κ^2-DPEphos)(NCMe)(H)(C(O)C$_6$H$_4$SMe)][CB$_{11}$H$_{12}$].[13] Aldehyde C−H activation is reversible at 298 K, as addition of **1b** to **3a** rapidly (time of mixing, less than 5 min) generates a ca. 1:1 mixture of **3a**,**b** alongside **1a**,**b** (Scheme 4). We have recently reported that both hydride insertion and C−H oxidative addition processes are reversible in linear-selective alkene hydroacylation reactions using **1a** and catalysts based upon small-bite-angle "PCP" ligand sets.[11]

The isolation of **6** demonstrates that hydride migration, rather than the alternative carbometalation, has occurred to give a branched intermediate.[35,48] To fully establish the role of **6** as an intermediate in alkyne hydroacylation, we have explored the reductive C−C bond-forming reaction to produce the branched product **5**. This process is not fast at 298 K, taking approximately 5 days to go to completion. However, heating a d_6-acetone solution of **6** to 323 K for 8 h resulted in the quantitative formation of a single product, that of reductive C−C bond formation: [Rh(*cis*-κ^2-DPEphos)(η^2:η^2,κ^1-H$_2$C═C(Ar^F)C(═O)(C$_6$H$_4$SMe)][CB$_{11}$H$_{12}$] (**7**) (Scheme 5). Complex **7** can also be prepared from addition of **5** to [Rh(*cis*-κ^2-DPEphos)(acetone)$_2$][CB$_{11}$H$_{12}$]. Figure 2 shows the molecular structure of the cation, as obtained from a single-crystal X-ray diffraction study. This demonstrates that it is has a pseudo-trigonal-bipyramidal coordinated Rh(I) center, in which the DPEphos adopts a *cis*-κ^2P,P coordination mode (Rh1−O2 = 3.395(5) Å) and the branched hydroacylation product **5** is bound in a tridentate fashion to the metal through η^2-alkene, η^2-carbonyl, and κ^1-SMe interactions. NMR data are fully consistent with this structure being retained in solution: the ^{31}P{^{1}H} NMR shows two doublets of doublets with large ^{103}Rh−^{31}P couplings (150 and 171 Hz), and the ^{1}H NMR spectrum shows the Rh-bound alkene protons shifted upfield from both **6** and free **5**, at δ 3.60 and 2.24. Addition of **1a** to **7** resulted in the liberation of free **5**, upon time of mixing, and the regeneration of **3a** (Scheme 5).

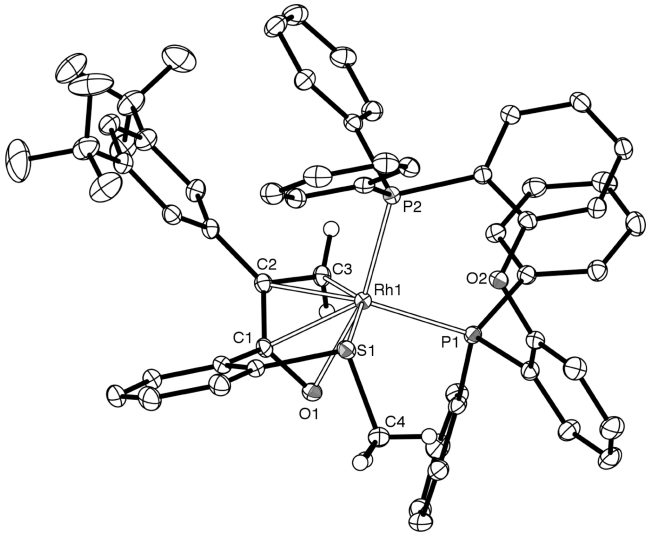

Figure 2. Displacement ellipsoid plot (30%) of complex **7**. Selected bond lengths (Å) and angles (deg): Rh1−P1, 2.3483(13); Rh−P2, 2.2810(13); Rh1−O1, 2.139(3); Rh1−C1, 2.148(5); Rh1−C2, 2.216(5); Rh1−C3, 2.123(5); Rh1−O1, 2.139(3); Rh1−S1, 2.4579(12); Rh1−O2, 3.395(5); P2−Rh1−O1, 166.49(10); P1−Rh1−P2, 97.87(5), S1−Rh1−P1, 106.30(4). The anion and the majority of the H atoms are not shown.

The formation of **7** from **6** followed first-order kinetics, as expected: k_{obs} = (6.14 ± 0.04) × 10^{-5} s^{-1} (324 K). This can be compared to the measured rate constant for ketone reductive elimination from (η-C$_5$Me$_4$CF$_3$)Rh(PMe$_3$)(σ-COCH$_2$CH$_2$SiMe$_3$)(C$_6$H$_4$Me), k_{obs} = 2.0 × 10^{-5} s^{-1} (323 K),[7] which is also similar to that determined in related Co systems.[12] Ketone formation from acyl-alkyl reductive elimination has been similarly measured in other systems.[49] Running the reaction at six different temperatures (303−238 K) allowed for an Eyring analysis (Supporting Information), from which $\Delta H^‡$ = 95 ± 2 kJ mol^{-1} and $\Delta S^‡$ = −32 ± 7 J K^{-1} mol^{-1} were determined: $\Delta G^‡$(298 K) = 105 ± 4 kJ mol^{-1}. The small but negative entropy of activation suggests an ordered transition state for reductive elimination and is consistent with an intramolecular process.[50] No linear product **4** was observed under these conditions, which is also consistent with insertion of the hydride into the alkyne being irreversible. Starting from *syn*-/*anti*-***d*-6** revealed a first-order rate constant of (5.50 ± 0.03) × 10^{-5} s^{-1}, corresponding to k_H/k_D = 1.1 ± 0.1. This negligible KIE is likely due to a secondary isotope effect. Krogh-Jespersen and Goldman have shown that reductive elimination of *trans*-stilbene from Ir(PCP)Ph(CH═CPhH) shows a

dx.doi.org/10.1021/om300647n | *Organometallics* 2012, 31, 5650−5659

Scheme 6

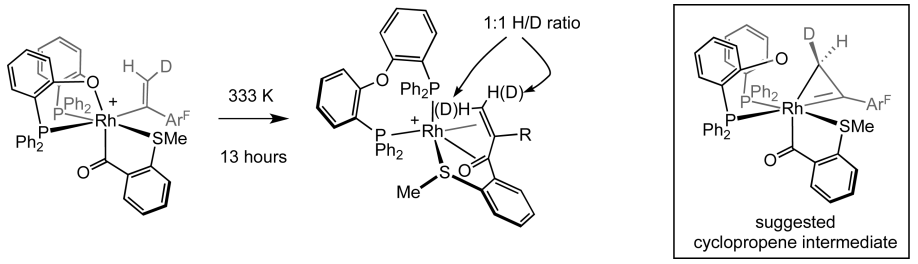

negative entropy of activation similar to that measured for **6**, but a lower enthalpy of activation.[50]

Heating (323 K) of the partially deuterated *anti*-***d*-6** revealed that an additional process was occurring before final reductive C−C bond formation of the final product, in which *anti*-***d*-6** underwent isomerization to give a mixture with *syn*-***d*-6**, so that the final product ***d*-7** has an approximately equal distribution of D into the two alkene positions (Scheme 6). Monitoring the ^{1}H NMR spectrum (323 K) with time showed an immediate reduction in intensity of the signal at δ 5.72 (*syn*-H), and the increase in the signal at δ 5.50 (*anti*-H), while at the same time signals due to both isotopomers of ***d*-7** are observed in the ^{2}H NMR spectrum. Related behavior is observed when starting from *syn*-***d*-6**. These observations are consistent with a degenerate equilibrium being established between these two isomers of **6**. We suggest that this isomerization could occur via a metallacyclopropene intermediate (Scheme 6), and such intermediates have been invoked to explain the apparent *trans* addition in intramolecular alkyne hydroacylation[26,36] and hydrosilylation of alkenes.[51−53] They have also been discussed in the context of *trans* hydroboration of alkynes.[54] The process here must have a barrier comparable to that of reductive elimination, as it does not occur at a significant rate at room temperature.

Attempts to prepare a complex bound with the linear product **4** by addition of independently prepared **4** to [Rh(*cis*-κ^2-DPEphos)(acetone)$_2$][$CB_{11}H_{12}$] immediately led to an equilibrium mixture of four products, one of which is the anticipated complex [Rh(*cis*-κ^2-DPEphos)(κ^2-(Ar^F)HC=CHC(=O)(C_6H_4SMe)][$CB_{11}H_{12}$] (**8**). The other three species are assigned to the isomeric products of C−S bond activation of **8**, [Rh(κ^3-DPEphos)(κ^2-(Ar^F)HC=CHC(=O)-(C_6H_4))(SMe)][$CB_{11}H_{12}$] (**9a−c**) (Scheme 7). Over time the *mer* isomer **9c** becomes the dominant species (greater than 90%), suggesting that it is thermodynamically preferred. These complexes have been identified by ^{31}P{^{1}H}, ^{1}H, ^{1}H−^{31}P HMBC, ^{1}H−^{1}H COSY, and ESI-MS experiments. These same four complexes are also observed on the stoichiometric (1:1) addition of **2** to **3a** (Scheme 2), which also forms **6** with ∼35% relative conversion. Addition of aldehyde **1a** to the **8**/**9a−c** mixture forms **3a** and liberates 1 equiv of **4** (Scheme 8). Addition of branched product **5** results in the appearance of additional signals due to free **4** and the coordinated branched product **7** (3:5 ratio, respectively). This demonstrates that equilibrium is established between bound **4** and bound **5**, with the branched isomer marginally favored. We have recently reported similar reversible C−S bond cleavage in β-S-substituted ketones using the [Rh(DPEphos)]$^+$ system as part of a carbothiolation strategy for functional group recycling and showed that a *mer* intermediate similar to **9c** was formed as an intermediate, which is in equilibrium with the simple ketone

Scheme 7

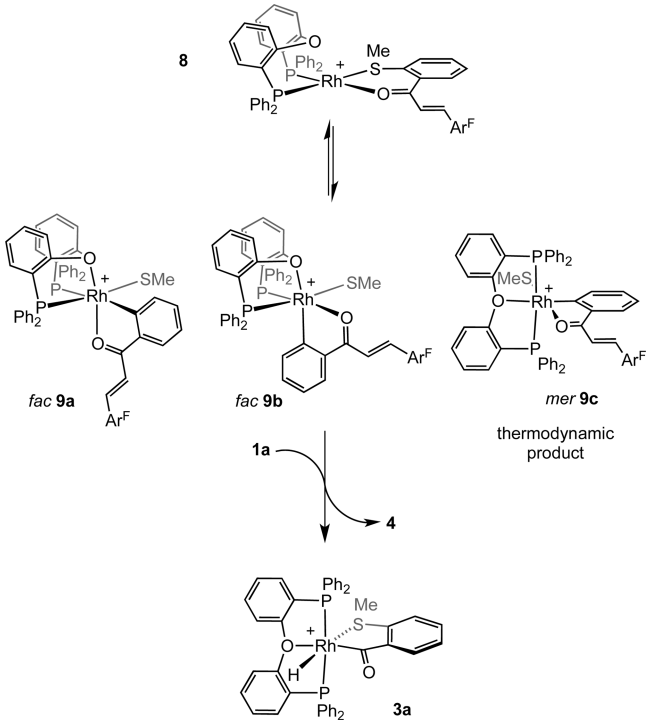

adduct.[55] However, we see no evidence for the competitive carbothiolation reaction between the linear alkenyl hydroacylation products and additional alkyne, as reaction with **1a** (to re-form **3a**) is clearly competitive with the reaction of C−S bond cleavage products with **2**. We do not see evidence for significant cyclotrimerization of the alkyne **2**,[56] which we have previously reported to be mediated by [Rh(DPEphos)]$^+$.[55] This process is also clearly not competitive with the productive hydroacylation reaction.

Combining our observations on the reaction of **1a** with **2** as mediated by [Rh(*cis*-κ^2-DPEphos)(acetone)$_2$][$CB_{11}H_{12}$] leads to the reaction pathway presented in Scheme 8. Addition of **1a** to the precursor acetone complex results in rapid oxidative addition to give **3a**, that then—via a hemilabile DPEphos ligand action—coordinates alkyne (**F**). This common intermediate undergoes hydride insertion to give either linear (**G**, unobserved) or branched (**6**) acyl-alkenyl intermediates. Partitioning at this stage is approximately 1:2 in favor of the linear. Reductive C−C bond formation gives the product-bound complexes **7** or **8**, which then can turnover on addition of more **1a** to give **3a**. That reaction of **3a** with excess **1a**/**2** produces **4**/**6** but no **5** (Scheme 2) indicates that the reductive C−C bond formation is lower in energy for the linear than for the branched pathway and once **6** does form it sits in a rather

dx.doi.org/10.1021/om300647n | *Organometallics* 2012, 31, 5650−5659

Scheme 8

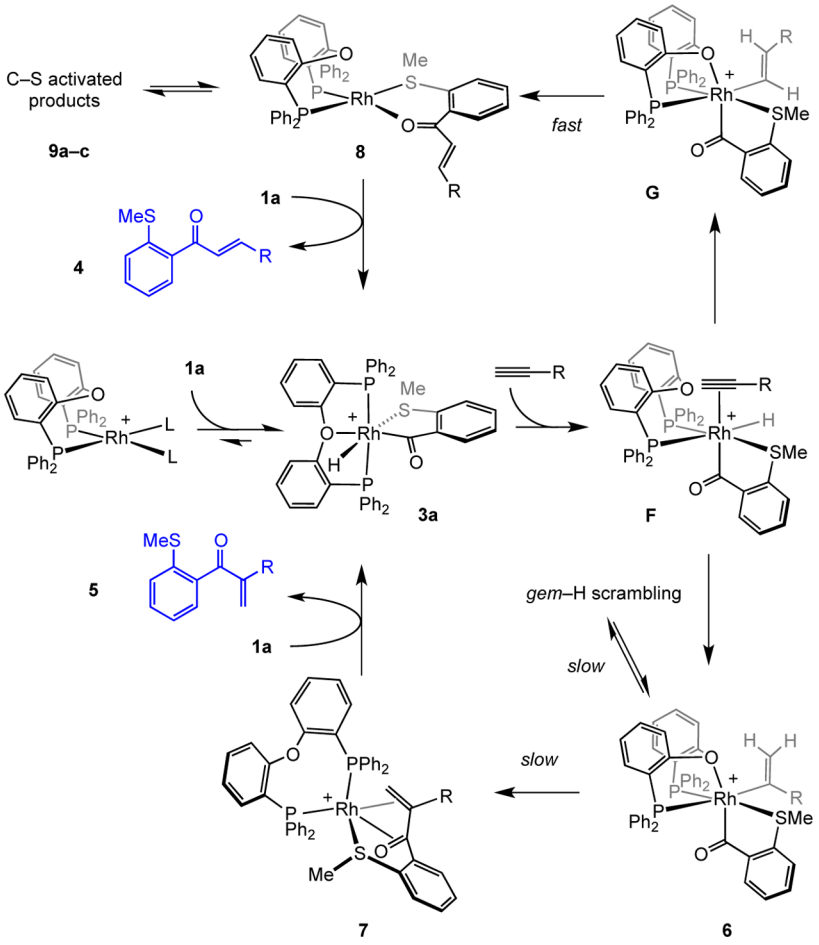

deep energy well and undergoes C–C bond formation slowly. This means that once **6** pools after a few turnovers, becoming the resting state, its turnover becomes effectively rate controlling for the whole system under catalytic conditions. Figure 3 shows time–concentration plots for catalysis at 323 K and effective 10 mol % loadings using [Rh(*cis*-κ^2-DPEphos)(acetone)$_2$][$CB_{11}H_{12}$] and **6** as catalysts. Starting from **6**, under these conditions of catalytic turnover, both a pseudo-zero-order consumption of substrates and formation of products is observed, with the rates of formation of **4** and **5** being (1.97 ± 0.03) × 10^{-6} and (1.03 ± 0.01) × 10^{-6} M s^{-1}, respectively, and the rates of consumption of **1a** and **2a** being (2.91 ± 0.05) × 10^{-6} and (2.63 ± 0.03) × 10^{-6} M s^{-1}, respectively. That the relative rates of product formation of both **4** and **5** display pseudo-zero-order kinetics suggests that the hydride insertion step for both pathways is not significantly reversible, in line with our empirical observations. Starting from [Rh(*cis*-κ^2-DPEphos)(acetone)$_2$][$CB_{11}H_{12}$] initially shows the very rapid formation of **4** (approximately 2 equiv relative to Rh) and then the slower growth in of **4** and **5**, again following pseudo-zero-order kinetics, with rates very similar to those when starting with **6**: e.g. (1.75 ± 0.03) × 10^{-6} M s^{-1} (**4**) and (0.96 ± 0.07) × 10^{-6} M s^{-1} (**5**). Starting from **3a** produces essentially the same time–concentration profile. At room temperature (298 K) the reaction is considerably slower but still follows zero-order kinetics. Starting from ***d*-1a/2** (10 mol % **6**, 323 K) resulted in no significant change in the observed rates. Both D isotopomers of **5** were observed (Scheme 6) but only one of **4** (*β*-*d*-**4**, Scheme 4) in this experiment. During catalysis **6** is the only observed organometallic species under all conditions. However, on consumption of all of **1a** and **2** the **7**/**8**/**9a–c** mixture then evolves, consistent with our stoichiometric studies.

Kinetic modeling supports our proposed mechanism, with the rate constant for reductive elimination from **6a** comparing well with experiment (modeled, 5.6(2) × 10^{-5} s^{-1}; experiment, 6.14(4) × 10^{-5} s^{-1}). When starting from [Rh(*cis*-κ^2-DPEphos)(acetone)$_2$][$CB_{11}H_{12}$], extrapolation of the steady-state evolution of **4** back to t = 0 (Figure 3) affords a y intercept corresponding to $[Rh]_{TOT} \times k_{rel}$, where k_{rel} is the partitioning at the hydride insertion step between **G** and **6**. This is 1.86(7) in favor of the linear pathway at 323 K, also consistent with our experimental observations. The early-phase temporal evolution of the linear product **4** (Figure 3, top) indicates that reductive elimination from the linear intermediate (i.e., **G**) is substantially faster than in branched **6**; simulation affords a threshold relative rate of ≥360, although the real value may be orders of magnitude higher. Moreover, the sum of the rates of evolution of linear and branched products (2.71 × 10^{-6} M s^{-1} at 0.018 M $[Rh]_{TOT}$) corresponds well with the partitioning-normalized rate of reductive elimination ($(1 + k_{rel})k_{obs}[Rh]_{TOT}$) of the branched isomer from **6a**, this then being the turnover-limiting step in the overall catalytic cycle presented in Scheme 8.

That the reductive C–C bond formation has a higher barrier for the branched intermediate (**6** is observed during catalysis but linear **4** is produced more rapidly) echoes related

dx.doi.org/10.1021/om300647n | *Organometallics* 2012, 31, 5650–5659

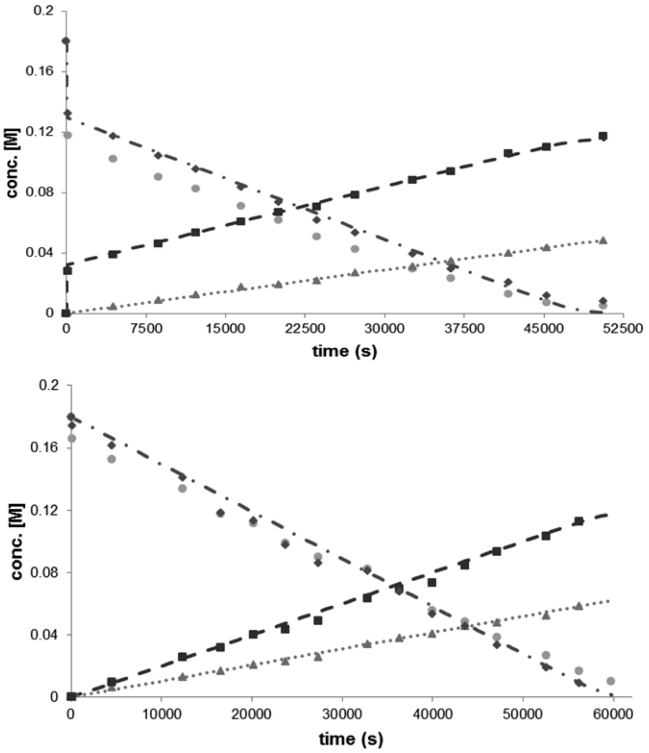

Figure 3. Time−concentration plots for catalysis. Conditions: 323 K; acetone solvent; [**1a**] = [**2**] = 0.18 M; (top) catalyst [Rh(*cis*-κ^2-DPEphos)(acetone)$_2$][$CB_{11}H_{12}$], 0.018 M; (bottom) catalyst **6**, 0.018 M. Legend: (●) **1a**; (♦) 2; (■) **4**; (▲) **5**. Dashed lines refer to the kinetic model (see the Supporting Information).

experimental and DFT studies on systems such as Ir(PCP)Ph(CH═CPhH) by Krogh-Jespersen and Goldman.[50] These studies show that before productive C−C bond formation the vinyl group has to undergo a 90° twist from its ground-state orientation so that the nascent C−C bond is approximately perpendicular to the vinyl plane, giving a "face-on" orientation between the coupling groups. This orientation minimizes steric resistance during the sp^2−sp^2 reductive coupling. For **6** this would entail a twist of the alkenyl group around the Rh1−C1 axis to place it approximately collinear with Rh−P2 (Figure 1). Although we only have data for the branched intermediate **6** and can only speculate on the structure of the associated linear intermediate (**G**, Scheme 8), that the linear final product **4** is produced rapidly suggests the barrier to C−C bond formation must be much lower from the corresponding intermediate. This could be due to favorable sterics, and evidence for this comes from studies on reductive elimination in linear and branched isomers of Ir(PCP)(CCPh)(R) (R = e.g. CPh═CH_2, CH═CPh) to form enyne organic products. These show that steric crowding in branched intermediates inhibits C−C reductive elimination, even though such species are higher in energy than their linear analogues, as rotation of the vinyl group to the appropriate orientation is inhibited by steric crowding in the branched isomers.[42] Brookhart and co-workers have reported a similar analysis for the sp^3−sp^2 reductive elimination in Ir-pincer complexes.[57]

■ CONCLUSIONS

The isolation of the branched alkenyl intermediate **6**, which directly precedes reductive elimination of the final ketone product, in the hydroacylation reaction between an alkyne and β-S-substituted aldehydes allowed for the mechanism of this important reaction to be probed in detail. The structure of **6** shows that, in this system at least, hydride migration rather than acyl migration occurs, while the elucidation of activation parameters for the subsequent reductive elimination is a first for the most commonly used set of catalysts used in this transformation: those based upon [Rh(chelating phosphine)]$^+$. Mechanistic studies show that, in contrast to alkene hydroacylation, hydride insertion into the alkyne is not reversible and also reveal an interesting isomerization process is occurring between the two branched alkenyl protons. Moreover, the observation of both linear and branched products under stoichiometric and catalytic regimes, in combination with kinetic modeling, allows for insight into the underlying reasons behind the selectivity of this reaction. In this system reductive elimination is much faster from the linear alkenyl intermediate than from the branched (at least 300 times faster), while hydride insertion to give the linear product is also modestly favored. An explanation for the large difference in reductive elimination, as recently outlined by others for related systems,[42,57] comes from the observation that steric crowding in branched intermediates can slow C−C reductive elimination, even though such species are higher in energy than their linear analogues, if the rotation of the vinyl group to the appropriate orientation is inhibited by steric crowding in the branched isomers. Interestingly, we have recently shown that systems using the ligands (o-^{i}PrC$_6$H$_4$)$_2$PCH$_2$CH$_2$P(o-^{i}PrC$_6$H$_4$)$_2$ promote excellent branched selectivity, while Cy$_2$PCH$_2$CH$_2$PCy$_2$ gives excellent linear selectivity, for the coupling of **1a** and **2**.[33] Thus, subtle variations of ligand sterics (and electronics) can switch the productive pathway, and these could well involve ligand-enforced changes to the relative barriers to reductive elimination on the basis of the arguments above. Understanding in detail why each ligand set promotes one pathway over the other will be an important next step on the road to delivering a truly general hydroacylation reaction for a broad range of substrates through manipulation of the complete catalytic cycle.

■ EXPERIMENTAL SECTION

General Experimental Procedures. All manipulations, unless otherwise stated, were performed under an atmosphere of argon, using standard Schlenk-line and glovebox techniques. Glassware was oven-dried at 130 °C overnight and flamed under vacuum prior to use. CH_2Cl_2, MeCN, hexane, and pentane were dried using a Grubbs-type solvent purification system (MBraun SPS-800) and degassed by successive freeze−pump−thaw cycles.[58] C_6H_5F was distilled under vacuum from CaH_2 and stored over 3 Å molecular sieves.[59] Acetone and d_6-acetone were dried over Ba_2O_3 and vacuum-distilled twice. NMR spectra were recorded on Varian Unity 500 MHz, Varian Mercury 300 MHz, Varian Venus 300 MHz, Bruker DRX 500, and Bruker AVC 500 MHz spectrometers at room temperature, unless otherwise stated. Chemical shifts are quoted in ppm and coupling constants in Hz. ESI-MS were recorded on a Bruker MicrOTOF instrument.[60] The starting materials, Cs[$CB_{11}H_6Br_6$],[61] Cs[$CB_{11}H_{12}$],[62] [Rh(NBD)(DPEphos)][X][13] (where [X]$^-$ = [$CB_{11}H_6Br_6$]$^-$, [$CB_{11}H_{12}$]$^-$), [Rh(DPEphos)(acetone)2][X],[13] [Rh(DPEphos)(H)(COC_6H_4SMe)][X],[13] and aldehyde **1b**,[18] were all prepared by published literature methods or variations thereof using Cs[$CB_{11}H_6Br_6$] or Cs[$CB_{11}H_{12}$] as the chloride extracting agent for the organometallic complexes. Aldehyde **1a** was obtained from a commercial source and purified by distillation before use. All other chemicals are commercial products and were used as received. Microanalyses were performed by Elemental Microanalysis Ltd. or London Metropolitan University.

dx.doi.org/10.1021/om300647n | *Organometallics* 2012, 31, 5650−5659

Synthesis of New Complexes. *[Rh(fac-κ³P,O,P-DPEphos){κ²C,S-C(O)C$_6$H$_4$SCH$_3$}{C(=CH$_2$)C$_6$H$_3$(CF$_3$)$_2$}][CB$_{11}$H$_{12}$] (**6**).* [Rh(DPEphos)(acetone)$_2$][CB$_{11}$H$_{12}$] was formed in situ on hydrogenation (4 atm) of [Rh(DPEphos)NBD][CB$_{11}$H$_{12}$] (100.9 mg, 0.12 mmol, 1 equiv) in acetone (5 mL). Aldehyde HC(O)C$_6$H$_4$SMe (**1a**; 74.2 μL, 0.6 mmol, 5 equiv) and alkyne HC≡CC$_6$H$_3$(CF$_3$)$_2$ (**2**; 101.8 μL, 0.6 mmol, 5 equiv) were added, and the solution was stirred for 1 h. There was a color change from dark red through dark brown and finally to bright yellow. The solution was added dropwise to a stirred solution of pentane (30 mL) to give a suspension of a pale solid in bright yellow solution. The solution was filter-decanted off and the solid washed with pentane (5 × 5 mL). The resulting off-white solid was dried in vacuo (yield 86%, 117 mg).

^{1}H NMR (500 MHz, d_6-acetone): δ 8.53 [app dd, 1H, J(HH) = 8.1, J(PH) = 4.9, Ar H], 8.34 [app dd, 1H, J(HH) = 8.5, J(PH) = 5.3, Ar H], 8.09−8.00 (m, 4H, Ar−H), 7.80−7.24 (m, 20H, Ar H), 7.12 [app t, 1H, J = 7.6, Ar H], 7.02 [app t, 1H, J = 7.4, Ar H], 6.94 [app d, 1H, J = 7.8, Ar H], 6.65 [app td, 2H, J = 8.2, J(PH) = 2.6, Ar H], 6.42 (s, 2H, Ar H), 6.30 [app ddd, 2H, J(PH) = 10.9, J = 8.2, J = 1.0, Ar H], 5.72 [d, 1H, J(PH) = 8.9, C=CH$_2$], 5.50 [d, 1H, J(PH) = 18.1, C=CH$_2$′], 2.59 (br s, 3H, S-CH$_3$), 2.27−1.11 (br m, 12H, CB$_{11}$H$_{12}$). ^{31}P{^{1}H} NMR (202 MHz, d_6-acetone): δ 21.87 [dd, J(RhP) = 166.5, J(PP) = 27.0], 13.12 [dd, J(RhP) = 78.7, J(PP) = 27.0]. ^{19}F NMR (282 MHz, d_6-acetone): δ 62.92 (br s, fwhm =2.6, CF$_3$). ^{1}H{^{31}P-(selective 22 ppm)} NMR (500 MHz, d_6-acetone, selected data): δ 8.34 [app d, 1H, J = 8.5, Ar H], 2.59 (sharp s, 3H, S-CH$_3$). ^{1}H{^{31}P(selective 13 ppm} NMR (500 MHz, d_6-acetone, selective data): δ 8.53 [app d, 1H, J(HH) = 8.1, Ar H], 6.65 [app t, 2H, J = 8.2, Ar H], 6.30 [app dd, 2H, J = 8.2, J = 1.0, Ar H], 5.72 (s, C=CH$_2$), 5.50 (s, C=CH$_2$′). ^{1}H−^{1}H COSY NMR (500 MHz, d_6-acetone): correlation observed between C=CH$_2$ proton signals at δ 5.72 and 5.50. ^{1}H−^{13}C HSQC NMR (500 MHz, d_6-acetone): two ^1J(CH) environments are observed for the C=CH$_2$ protons, to the same carbon (δ 122.2). ESI-MS (fluorobenzene, 60 °C, 4.5 kV, positive ion): [M]$^+$ m/z 1031.1497 (calcd 1031.1178). Anal. Calcd for C$_{55}$H$_{52}$B$_{11}$F$_6$O$_2$P$_2$RhS (1174.8291): C, 56.23; H, 4.46. Found: C, 56.31; H, 4.44.

*[Rh(fac-κ³P,O,P-DPEphos){κ²C,S-C(O)C$_6$H$_4$SCH$_3$}{C(C=D$_2$)-C$_6$H$_3$(CF$_3$)$_2$}][CB$_{11}$H$_6$Br$_6$] (**d$_2$-6**).* The complex was synthesized according to the method above (using ***d*-1a** and ***d*-2**) to give an off-white solid (yield 93%, 24.6 mg). NMR characterization showed the same spectrum as for **6**, except for selected data, shown below.

^{2}H NMR (76.7 MHz, acetone): δ 5.72 (s, CD$_2$), 5.54 (s, CD$_2$′).

*[Rh(fac-κ³P,O,P-DPEphos){κ²C,S-C(O)C$_6$H$_4$SCH$_3$}{C(C=DH)-C$_6$H$_3$(CF$_3$)$_2$}][CB$_{11}$H$_6$Br$_6$] (anti-**d-6**).* The complex was synthesized according to the method above (with **1a** and ***d*-2**) to give an off-white colored solid (yield =96%, 18.0 mg). NMR characterization showed the same spectrum as for **6**, except for selected data, shown below.

^{1}H NMR (500 MHz, acetone, selected data): δ 5.72 [d, 1H, J(PH) = 8.9, C=CHD]. ^{2}H NMR (76.7 MHz, acetone): δ 5.60 (s, CHD). Anal. Calcd for C$_{55}$H$_{51}$B$_{11}$F$_6$O$_2$P$_2$RhS (1175.83): C, 56.18; H, 4.54. Found: C, 56.27; H, 4.42.

*[Rh(fac-κ³P,O,P-DPEphos){κ²C,S-C(O)C$_6$H$_4$SCH$_3$}{C(C=HD)-C$_6$H$_3$(CF$_3$)$_2$}][CB$_{11}$H$_6$Br$_6$] (syn-**d-6**).* The complex was synthesized according to the method above (with ***d*-1a** and **2**) to give an off-white solid (yield 87%, 19.7 mg). NMR characterization showed the same spectrum as for **6**, except for selected data, shown below.

^{1}H NMR (500 MHz, acetone, selected data): δ 5.50 [d, 1H, J(PH) = 18.1, C=CDH]. ^{2}H NMR (76.7 MHz, acetone): δ 5.73 (s, CDH).

*[Rh(fac-κ³P,O,P-DPEphos){κ³-C$_6$H$_3$(CF$_3$)$_2$C(=CH$_2$)C(O)C$_6$H$_4$SCH$_3$}][CB$_{11}$H$_{12}$] (**7**).* The isolated branched product C$_6$H$_3$(CF$_3$)$_2$C(=CH$_2$)C(O)C$_6$H$_4$SCH$_3$ (**5**; 7.4 mg, 0.018 mmol, 1 equiv) was added to a solution of [Rh(DPEphos)(acetone)$_2$][CB$_{11}$H$_{12}$] (16.6 mg, 0.018 mmol, 1 equiv) in CH$_2$Cl$_2$ (5 mL). A color change from dark red to orange-yellow was observed, while the mixture was stirred for 1 h. Crystals suitable for X-ray diffraction were obtained by diffusion of pentane into a solution of the complex in CH$_2$Cl$_2$ (yield 87%, 15.8 mg).

^{1}H NMR (500 MHz, d_6-acetone): δ 7.91−7.05 [m, 31H, {7.34 [td, 2H, J = 7.8, J(PH) = 2.1], 7.29 (t, 1H, J = 8.0), 7.15 [app dd, 1H, J = 7.5, J(PH) = 5.3], 7.08 (t, 1H, J = 9.0)}, 6.94 [app dd, 2H, J(PH) = 11.7, J = 7.5, Ar H], 6.78 [t, 1H, J = 7.5, Ar H], 6.39 [app dd, 1H, J(PH) = 10.5, J = 7.5, Ar H], 3.60 (br s, 1H, C=CH$_2$), 2.25 [app ddt, 1H, J(PH) = 11.5, J(PH) = 1.5, J = 1.65, C=CH$_2$′], 2.24−1.11 (m, 12H, CB$_{11}$H$_{12}$), 1.93 (s, 3H, S-CH$_3$). ^{31}P{^{1}H} NMR (202 MHz, d_6-acetone): δ 31.65 [dd, J(RhP) = 151.5, J(PP) = 38.4], 27.90 [dd, J(RhP) = 171.0, J(RhP) = 39.1]. ^{1}H{^{31}P} NMR (500 MHz, d_6-acetone, selected data): δ 2.25 [app t, J = 1.65, C=CH$_2$′]. ^{1}H{^{31}P-selective 32 ppm} NMR (500 MHz, d_6-acetone, selected data): δ 7.34 (t, 2H, J = 7.8, Ar H), 7.15 (app d, 1H, J = 7.5, Ar H), 6.94 (app d, 2H, J = 7.5, Ar H), 6.39 (app d, 1H, J = 7.5, Ar H), 3.60 (sharp s, 1H, C=CH$_2$), 2.25 [app dt, 1H, J(PH) = 11.5, J = 1.65, C=CH$_2$′]. ^{1}H{^{31}P-selective 28 ppm} NMR (500 MHz, d_6-acetone, selected data): δ 7.08 (app d, 1H, J = 7.5, Ar H), 2.25 (m, 1H, C=CH$_2$′). ^{1}H−^{1}H COSY NMR (500 MHz, d_6-acetone): correlation observed between C=CH$_2$ proton peaks. ^{1}H−^{13}C HSQC NMR (500 MHz, d_6-acetone): correlation observed between C=CH$_2$ peaks, on the same carbon. ESI-MS (fluorobenzene, 60 °C, 4.5 kV, positive ion): [M]$^+$ m/z 1031.1505 (calcd 1031.8021).

*[Rh(cis-κ²P,P-DPEphos){κ²O,S-SCH$_3$C$_6$H$_4$O(C)C(=CH$_2$)-C$_6$H$_3$(CF$_3$)$_2$}][CB$_{11}$H$_{12}$] (**8**), [Rh(fac-κ³P,O,P-DPEphos)(SCH$_3$){κ²C,O-C$_6$H$_4$C(O)CHCHC$_6$H$_3$(CF$_3$)$_2$}][CB$_{11}$H$_{12}$] (**9a,b**), and [Rh(mer-κ³(POP)-DPEphos)(SCH$_3$){κ²C,O-C$_6$H$_4$C(O)CHCHC$_6$H$_3$(CF$_3$)$_2$}][CB$_{11}$H$_{12}$] (**9c**).* The title compounds are formed in situ on addition of isolated linear product (4) C$_6$H$_3$(CF$_3$)$_2$CHCHC(O)C$_6$H$_4$SCH$_3$ (4.9 mg, 0.01 mmol, 1 equiv) to a solution of [Rh(DPEphos)(acetone)$_2$][CB$_{11}$H$_{12}$] (11.4 mg, 0.01 mmol, 1 equiv) in d_6-acetone (0.4 mL). A color change from dark red to dark brown was observed. The compound was characterized by NMR spectroscopy and ESI-MS.

^{1}H NMR (500 MHz, d_6-acetone, 293 K, selected data): δ 2.46 (s, S-CH$_3$, 8), 1.61 [br d, J = 6.9, S-CH$_3$, **9a**], 0.60 (s, S-CH$_3$, **9c**), −1.03 [br d, J = 5.4, S-CH$_3$, **9b**]. ^{31}P{^{1}H} NMR (202 MHz, d_6-acetone, 293 K): δ 47.01 [dd, J(RhP) = 148.3, J(PP) = 28.9, **9b**], 41.36 [dd, J(RhP) = 155.3, J(PP) = 38.6, **8**], 22.76 [dd, J(RhP) = 111.8, J(PP) = 28.5 Hz, **9b**], 19.84 [d, J(RhP) = 111.1, **9c**], 6.68 [dd, J(RhP) = 162.7, J(PP) = 38.6, **8**]. ^{31}P{^{1}H} NMR (202 MHz, d_6-acetone, 200 K): δ 48.58 [dd, J(RhP) = 147.5, J(PP) = 28.3, **9b**], 42.12 [dd, J(RhP) = 153.5, J(PP) = 38.4, **8**], 35.01 [dd, J(RhP) = 151.5, J(PP) = 24.2, **9a**], 23.97 [dd, J(RhP) = 107.1, J(PP) = 24.2, **9a**], 22.99 [dd, J(RhP) = 111.1, J(PP) = 28.3, **9b**], 20.13 [dd, J(RhP) = 111.1, J(PP) = 22.2, **9c**], 6.92 [dd, J(RhP) = 163.6, J(PP) = 40.4, **8**]. ESI-MS (fluorobenzene, 60 °C, 4.5 kV, positive ion): [M]$^+$ m/z 1031.1528 (calcd 1031.1178).

Crystallography. Relevant details about the structure refinements are given in Table S-1 (Supporting Information). Data for **3b**, **6**, and **7** were collected on an Enraf-Nonius Kappa CCD diffractometer using graphite-monochromated Mo Kα radiation (λ = 0.710 73 Å) and a low-temperature device;[63] data were collected using COLLECT, and reduction and cell refinement were performed using DENZO/SCALEPACK.[64] The structures were solved by direct methods using SIR92[65] and refined by full-matrix least-squares methods on F^2 using SHELXL-97.[66] All non-hydrogen atoms were refined with anisotropic displacement parameters. Hydrogen atoms were placed in calculated positions and refined using the riding model. Problematic solvent disorder in the structure of **6** was treated using SQUEEZE within PLATON.[67] Further details of disorder modeling are documented in the crystallographic information files under the heading _refine_special_details. Restraints to thermal parameters were necessary in order to maintain sensible values.

■ ASSOCIATED CONTENT

Supporting Information

Text, tables, figures, and CIF files giving full synthetic, crystallographic, and characterization details for **3b**, an Eyring analysis for **6**, and details of the kinetic modeling. This material is available free of charge via the Internet at http://pubs.acs.org. Crystallographic data have also been deposited with the Cambridge Crystallographic Data Center (CCDC: 882542, **3b**; 882543, **6**; 882544, **7**) and can be obtained via www.ccdc.cam.ac.uk/data_request/cif.

AUTHOR INFORMATION

Corresponding Author

*E-mail: andrew.weller@chem.ox.ac.uk.

Notes

The authors declare no competing financial interest.

ACKNOWLEDGMENTS

We acknowledge the University of Oxford (studentship to R.P.), the European Union (FP7, Marie Curie Action "Dehydrocouple", M.H.), Sarah-Jane Poingdestre (Oxford) for kindly providing the isolated products, and Robert J. Cox (Bristol) for experimental assistance. G.C.L.-J. is a Royal Society Wolfson Research Merit Award holder.

REFERENCES

(1) Suggs, J. W. *J. Am. Chem. Soc.* **1978**, *100*, 640.
(2) Jun, C. H.; Jo, E. A.; Park, J. W. *Eur. J. Inorg. Chem.* **2007**, 1869.
(3) Willis, M. C. *Chem. Rev.* **2009**, *2010*, 725.
(4) Leung, J. C.; Krische, M. J. *Chem. Sci.* **2012**, *3*, 2202.
(5) Fairlie, D. P.; Bosnich, B. *Organometallics* **1988**, *7*, 946.
(6) Fairlie, D. P.; Bosnich, B. *Organometallics* **1988**, *7*, 936.
(7) Roy, A. H.; Lenges, C. P.; Brookhart, M. *J. Am. Chem. Soc.* **2007**, *129*, 2082.
(8) Lenges, C. P.; Brookhart, M. *J. Am. Chem. Soc.* **1997**, *119*, 3165.
(9) Omura, S.; Fukuyama, T.; Horiguchi, J.; Murakami, Y.; Ryu, I. *J. Am. Chem. Soc.* **2008**, *130*, 14094.
(10) Shibahara, F.; Bower, J. F.; Krische, M. J. *J. Am. Chem. Soc.* **2008**, *130*, 14120.
(11) Chaplin, A. B.; Hooper, J. F.; Weller, A. S.; Willis, M. C. *J. Am. Chem. Soc.* **2012**, *134*, 4885.
(12) Lenges, C. P.; White, P. S.; Brookhart, M. *J. Am. Chem. Soc.* **1998**, *120*, 6965.
(13) Moxham, G. L.; Randell-Sly, H.; Brayshaw, S. K.; Weller, A. S.; Willis, M. C. *Chem. Eur. J.* **2008**, *14*, 8383.
(14) Moxham, G. L.; Randell-Sly, H. E.; Brayshaw, S. K.; Woodward, R. L.; Weller, A. S.; Willis, M. C. *Angew. Chem., Int. Ed.* **2006**, *45*, 7618.
(15) Jun, C.-H.; Lee, H.; Hong, J.-B.; Kwon, B.-I. *Angew. Chem., Int. Ed.* **2002**, *41*, 2146.
(16) Coulter, M. M.; Dornan, P. K.; Dong, V. M. *J. Am. Chem. Soc.* **2009**, *131*, 6932.
(17) Coulter, M. M.; Kou, K. G. M.; Galligan, B.; Dong, V. M. *J. Am. Chem. Soc.* **2010**, *132*, 16330.
(18) González-Rodríguez, C.; Pawley, R. J.; Chaplin, A. B.; Thompson, A. L.; Weller, A. S.; Willis, M. C. *Angew. Chem., Int. Ed.* **2011**, *50*, 5134.
(19) Osborne, J. D.; Randell-Sly, H. E.; Currie, G. S.; Cowley, A. R.; Willis, M. C. *J. Am. Chem. Soc.* **2008**, *130*, 17232.
(20) Hoffman, T. J.; Carreira, E. M. *Angew. Chem., Int. Ed.* **2011**, *50*, 10670.
(21) Shibata, Y.; Tanaka, K. *J. Am. Chem. Soc.* **2009**, *131*, 12552.
(22) Tanaka, K.; Shibata, Y.; Suda, T.; Hagiwara, Y.; Hirano, M. *Org. Lett.* **2007**, *9*, 1215.
(23) Shen, Z.; Dornan, P. K.; Khan, H. A.; Woo, T. K.; Dong, V. M. *J. Am. Chem. Soc.* **2009**, *131*, 1077.
(24) Murphy, S. K.; Coulter, M. M.; Dong, V. M. *Chem. Sci.* **2012**, *3*, 335.
(25) Hyatt, I. F. D.; Anderson, H. K.; Morehead, A. T.; Sargent, A. L. *Organometallics* **2008**, *27*, 135.
(26) Chung, L. W.; Wiest, O.; Wu, Y. D. *J. Org. Chem.* **2008**, *73*, 2649.
(27) Meng, Q. X.; Shen, W.; He, R. X.; Li, M. *Transition Met. Chem.* **2011**, *36*, 793.
(28) Suggs, J. W.; Jun, C. H. *J. Chem. Soc., Chem. Commun.* **1985**, 92.
(29) Wentzel, M. T.; Reddy, V. J.; Hyster, T. K.; Douglas, C. J. *Angew. Chem., Int. Ed.* **2009**, *48*, 6121.
(30) Lutz, J. P.; Rathbun, C. M.; Stevenson, S. M.; Powell, B. M.; Boman, T. S.; Baxter, C. E.; Zona, J. M.; Johnson, J. B. *J. Am. Chem. Soc.* **2011**, *134*, 715.
(31) Jun and co-workers have suggested a carbometalation step to explain the formation of the branched regioisomer in the chelation-assisted hydroacylation of 1-hexyne with benzaldehyde.[2]
(32) Tanaka, M.; Imai, M.; Yamamoto, Y.; Tanaka, K.; Shimowatari, M.; Nagumo, S.; Kawahara, N.; Suemune, H. *Org. Lett.* **2003**, *5*, 1365.
(33) Poingdestre, S.-J.; Goodacre, J. D.; Weller, A. S.; Willis, M. C. *Chem. Commun.* **2012**, *48*, 6345.
(34) Pawley, R. J.; Moxham, G. L.; Dallanegra, R.; Chaplin, A. B.; Brayshaw, S. K.; Weller, A. S.; Willis, M. C. *Organometallics* **2010**, *29*, 1717.
(35) Wentzel, M. T.; Reddy, V. J.; Hyster, T. K.; Douglas, C. J. *Angew. Chem., Int. Ed.* **2009**, *48*, 6121.
(36) Tanaka, K.; Fu, G. C. *J. Am. Chem. Soc.* **2001**, *123*, 11492.
(37) Tanaka, K.; Fu, G. C. *J. Am. Chem. Soc.* **2003**, *125*, 8078.
(38) Tanaka, K.; Fu, G. C. *Angew. Chem., Int. Ed.* **2002**, *41*, 1607.
(39) Jeffrey, J. C.; Rauchfuss, T. B. *Inorg. Chem.* **1979**, *18*, 2658.
(40) Braunstein, P.; Naud, F. *Angew. Chem., Int. Ed.* **2001**, *40*, 680.
(41) The anion can be changed between $[CB_{11}H_{12}]^-$ and $[CB_{11}H_6Br_6]^-$ without affecting the chemistry. The choice of anion is dictated by the ease of crystallization of the resulting salt. See: Reed, C. A. *Chem. Commun.* **2005**, 1669.
(42) Ghosh, R.; Zhang, X.; Achord, P.; Emge, T. J.; Krogh-Jespersen, K.; Goldman, A. S. *J. Am. Chem. Soc.* **2007**, *129*, 853.
(43) Weng, W.; Parkin, S.; Ozerov, O. V. *Organometallics* **2006**, *25*, 5345.
(44) Portnoy, M.; Milstein, D. *Organometallics* **1994**, *13*, 600.
(45) Poulton, J. T.; Sigalas, M. P.; Eisenstein, O.; Caulton, K. G. *Inorg. Chem.* **1993**, *32*, 5490.
(46) Foo, T.; Bergman, R. G. *Organometallics* **1992**, *11*, 1811.
(47) A small amount of D incorporation into **7** was observed, but this was less than 5% by ^{1}H NMR spectroscopy.
(48) Di Giuseppe, A.; Castarlenas, R.; Pirez-Torrente, J. s. J.; Crucianelli, M.; Polo, V.; Sancho, R.; Lahoz, F. J.; Oro, L. A. *J. Am. Chem. Soc.* **2012**, *134*, 8171.
(49) Suggs, J. W.; Wovkulich, M. J.; Cox, S. D. *Organometallics* **1985**, *4*, 1101.
(50) Ghosh, R.; Emge, T. J.; Krogh-Jespersen, K.; Goldman, A. S. *J. Am. Chem. Soc.* **2008**, *130*, 11317.
(51) Tanke, R. S.; Crabtree, R. H. *J. Am. Chem. Soc.* **1990**, *112*, 7984.
(52) Jun, C.-H.; Crabtree, R. H. *J. Organomet. Chem.* **1993**, *447*, 177.
(53) Matsuda, T.; Ichioka, Y. *Org. Biomol. Chem.* **2012**, *10*, 3175.
(54) Cid, J.; Carbó, J. J.; Fernández, E. *Chem. Eur. J.* **2012**, *18*, 1512.
(55) Hooper, J. F.; Chaplin, A. B.; Gonzalez-Rodriguez, C.; Thompson, A. L.; Weller, A. S.; Willis, M. C. *J. Am. Chem. Soc.* **2012**, *134*, 2906.
(56) Saito, S.; Yamamoto, Y. *Chem. Rev.* **2000**, *100*, 2901.
(57) Bernskoetter, W. H.; Hanson, S. K.; Buzak, S. K.; Davis, Z.; White, P. S.; Swartz, R.; Goldberg, K. I.; Brookhart, M. *J. Am. Chem. Soc.* **2009**, *131*, 8603.
(58) Pangborn, A. B.; Giardello, M. A.; Grubbs, R. H.; Rosen, R. K.; Timmers, F. J. *Organometallics* **1996**, *15*, 1518.
(59) Burfield, D. R.; Smithers, R. H. *J. Org. Chem.* **1978**, *43*, 3966.
(60) Lubben, A. T.; McIndoe, J. S.; Weller, A. S. *Organometallics* **2008**, *27*, 3303.
(61) Liston, D. J.; Lee, Y. J.; Scheidt, W. R.; Reed, C. A. *J. Am. Chem. Soc.* **1989**, *111*, 6643.
(62) Shelly, K.; Finster, D. C.; Lee, Y. J.; Scheidt, W. R.; Reed, C. A. *J. Am. Chem. Soc.* **1985**, *107*, 5955.
(63) Cosier, J.; Glazer, A. M. *J. Appl. Crystallogr.* **1986**, *19*, 105.
(64) Otwinowski, Z.; Minor, W. In *Macromolecular Crystallography*; Carter, C. W., Jr., Sweet, R. M., Eds.; 1997; Part A, Vol. *276*.
(65) Altomare, A.; Cascarano, G.; Giacovazzo, G.; Guagliardi, A.; Burla, M. C.; Polidori, G.; Camalli, M. *J. Appl. Crystallogr.* **1994**, *27*, 435.
(66) Sheldrick, G. M. *Acta Crystallogr., Sect. A* **2008**, *64*, 112.
(67) Spek, A. L. *J. Appl. Crystallogr.* **2003**, *36*, 7.